ARTICLE

Formation of Straight 10 nm Diameter Silicon Nanopores in Gold Decorated Silicon

Claudia C. Büttner,[†,*] Andreas Langner,[‡] Markus Geuss,[§] Frank Müller, Peter Werner, and Ulrich Gösele

Max Planck Institute of Microstructure Physics, Weinberg 2, 06120 Halle, Germany. [†]Present address: German Aerospace Center, Linder Höhe, 51147 Köln, Germany. [‡]Present address: Paul Scherrer Institute, 5232 Villigen PSI, Switzerland. [§]Present address: Adolphe Merkle Institute, University of Fribourg, Rte de l'Ancienne Papeterie,1723 Marly, Switzerland.

ABSTRACT We observe pore formation with diameters in the 10 nm range in silicon when it is covered with gold particles. This pore etching occurs when the sample is put in 5 wt % hydrofluoric acid (HF) solution for a few minutes. The pores form along the ⟨100⟩ direction, which is also the preferred direction of macro- and mesopores electrochemically etched into silicon. No etching occurs if the dissolved oxygen is removed from the aqueous HF solution or the gold is removed from the silicon surface. This leads to the assumption that the dissolved oxygen acts as an oxidant as in the case of stain etching with gold as cathodic material. A tentative model is suggested to explain why all of the observed nanopores have roughly the same diameter of about 10 nm. These pores can occur for inhomogeneously gold-covered planar silicon surfaces but also in MBE (molecular beam epitaxy) grown silicon nanowires since these nanowires are covered unintentionally with gold nanoclusters at their cylindrical surface.

KEYWORDS: silicon · nanopores · HF · gold

Silicon is the main base material for micro- and nanoelectronics as well as photovoltaics. Silicon compared to other semiconductor materials such as Ge or GaAs is a rather inexpensive material. In addition, a technologically important oxide can be produced easily on the surface of silicon. Silicon is a potential material for optical applications, for example, as photonic crystals[1−4] as well as templates in materials science.[5−7] In most of these applications additional functionality to the silicon is given by using it in a porous form. Several processes are known to create various forms of porous silicon. One method, which leads to macroporous silicon, is based on a wet electrochemical etching process.[8] Silicon gets anodized and a platinum electrode works as a cathode. The most common electrolyte for the etching process is hydrofluoric acid (HF). Holes (h^+) in silicon are necessary for the anodic dissolution of silicon in HF. An anisotropic pore formation along the ⟨100⟩ direction as the preferred formation direction occurs if the chemical reaction is limited by charge transfer over the interface between silicon and HF solution.[9] According to Lehmann[10] this divalent etching can be written as

$$Si + 4HF_2^- + h^+ \rightarrow SiF_6^{2-} + 2HF + H_2 + e^- \quad (1)$$

The strong polarizing effect of fluorine present in the HF solution weakens the silicon backbonds. Because of the presence of HF and H_2O the bonds are broken eventually and the silicon is removed from the bulk.[10] While the silicon atoms in the {100} plane are only weakly bound, the bonding is stronger in other crystal directions which leads to a directed pore formation along the ⟨100⟩ direction.[11] This scheme applies for macro- as well as mesopores electrochemically etched into silicon.

Furthermore, other processes are known to form pores in silicon without an external applied potential. Li and Bohn[12] presented a method for metal-assisted porous silicon formation. For this process (also often called by its historical name "stain etching") an oxidant such as H_2O_2 is needed. When the silicon surface is covered by a noncontinuous thin metal film mesoporous silicon can be obtained. The metal acts as a cathodic site. H_2O_2 is reduced to H_2O and two holes are injected into the valence band of silicon. These holes are used for the dissolution and pore formation of silicon.

Another metal-assisted approach was recently reported by Huang *et al.*[13,14] They used a lithographically defined silver mask on top of a silicon wafer for the controlled etching of silicon. Thereby, only the areas covered by the silver are etched perpendicular to the surface. In this catalytic approach the silver sinks with the dissolved silicon into the structure and thus the silver covers the bottom of the etched parts.

*Address correspondence to claudia.buettner@dlr.de.

Received for review July 17, 2009 and accepted September 8, 2009.

Published online September 17, 2009. 10.1021/nn900817d CCC: $40.75

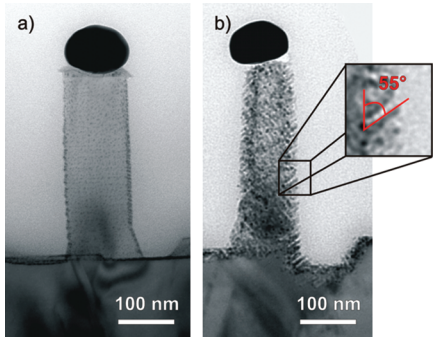

Figure 1. Comparison of (a) an as-grown MBE silicon nanowire and (b) a nanowire after an HF-dip (5 wt %, 3 min) which led to a corroded porous surface. The pores formed along the ⟨100⟩ direction, which is 55° to the ⟨111⟩ direction and the preferred electrochemical etching direction in silicon. The pictures are taken along ⟨110⟩ observation direction.

In our experiments, we observed an unexpected pore formation when silicon is in contact with gold and exposed to aqueous HF which is thus another metal-assisted etching process, but with clearly different features than discussed in the previous two sections.

RESULTS AND DISCUSSION

We first observed the unintended pore formation in molecular beam epitaxy (MBE) grown nanowires. In Figure 1 the TEM pictures display the difference between an as-grown MBE nanowire and an HF-treated one. The as-grown nanowire in Figure 1a has a smooth surface. The dark spots on the cylindrical wall are the gold clusters formed on the surface during the nanowire synthesis. After an HF-dip is performed the nanowire surface is porous and corroded as shown in Figure 1b. A pure chemical dissolution of the silicon can be excluded since the etching rate of HF for silicon is in the angstrom regime even after 3 min.[10] Furthermore, the nanowire shows a preferential direction of pore formation under a certain angle with respect to the surface. Form the magnified inset in Figure 1b it can be seen that the nanowire, which is imaged in ⟨110⟩ direction, exhibits pores at an angle of about 55° to the ⟨111⟩ growth direction. This corresponds to the ⟨100⟩ direction, which has an angle of 54.7° to the ⟨111⟩ direction. The ⟨100⟩ direction is the preferred etching direction during the divalent dissolution of silicon in HF (see eq 1). This pore formation also occurs on the surface of the silicon substrate. From the TEM images of the corroded nanowires no conclusion can be drawn whether the tiny gold clusters remained on the original surface or had moved into the material at the tip of the pores.

To exclude influences from the curved nanowire surface we also used planar pieces of silicon for the investigations. The planar silicon sample with the larger gold droplets also shows pores underneath the gold droplet after an HF-dip. In the TEM picture in Figure 2 ⟨100⟩ pores can be seen. The TEM sample is ⟨112⟩ oriented,

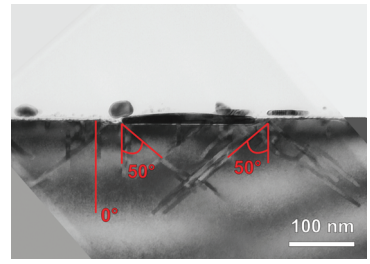

Figure 2. Planar silicon with gold droplets and pores reaching into the substrate along ⟨100⟩ direction after etching in 5 wt % HF for 3 min. The TEM sample is ⟨112⟩ oriented and ⟨100⟩ directions of the pores appear in their projection.

so that the ⟨100⟩ pores appear in their projection. From the sample orientation, an angle of 50.6° can be calculated for the projected ⟨100⟩ pores which is in excellent agreement with the measured angle of 50°. In the case of anodic dissolution of silicon in HF, pore growth in the ⟨113⟩ direction is reported as well for (111) silicon surfaces.[15] However, mesopore formation below a certain doping density seems to occur exclusively in ⟨100⟩ direction, independently of substrate orientation.[10]

In our experiments all pores have the same diameter of about 10 nm. The TEM pictures of the planar silicon samples show no gold particles at the bottom of the pores. Thus, a pore formation mechanism as proposed in ref 13 can be excluded in our case. However, the dark contrast of the pores in general indicates that the pore walls might be covered with a thin layer of gold. Since the occurrence of dark contrast phenomena at the pore walls might also be caused by special imaging condition without the presence of a separate metal layer, we tried to image the suspected gold layer by high resolution TEM imaging but got no conclusive results. This outcome indicates that the gold layer, if present at all, should only have a thickness in the range of one or a few monolayers. Further high resolution analytical methods will be required to prove or disprove unambiguously the presence of a thin gold layer at the pore walls. Therefore, the tentative model of the pore formation suggested below, which is based on the presence of a thin gold layer on the pore walls should be considered as speculative at the present stage.

The size of the pores has no relation to the size of the initial gold clusters. The pores are like the stain films described by Li and Bohn,[12] where porous silicon can be obtained out of a solution with HF and an oxidant such as H_2O_2. In our experiments the dissolved oxygen in the HF solution acts as an oxidant. Locally, an electrochemical dissolution of silicon takes place with silicon as the anode material and the gold works as the cathodic site. Furthermore, we observe a directional pore formation which indicates a divalent silicon dissolution reaction according to eq 1. For this process positive charge carriers are required in the silicon. Therefore, we propose the following mechanism for the silicon etching under our conditions:

Cathodic site:

$$\frac{1}{2}O_2 + 2H_3O^+ + 2e^- \rightarrow 3H_2O$$

Anodic site:

$$Si + 4HF_2^- + h^+ \rightarrow SiF_6^{2-} + 2HF + H_2 + e^-$$

Redox reaction:

$$\frac{1}{2}O_2 + 2H_3O^+ + Si + 4HF_2^- \rightarrow 3H_2O + SiF_6^{2-} + 2HF + H_2 \quad (2)$$

To confirm that the dissolved oxygen in the HF solution is responsible for the etching process, the oxygen was removed. Therefore, the HF solution was purged with nitrogen prior to the actual experiment. Next, the sample was put into the solution and the nitrogen was just flowing above the surface of the HF solution. Corresponding TEM investigations showed that those samples do not exhibit a mesoporous structure (Figure 3a). For comparison a porous nanowire is shown for which the oxygen was not removed before the HF-dip (Figure 3b). The nanowires where the dissolved oxygen was removed from the HF solution look like the as-grown nanowires. No pore formation could be detected at the surface which gives evidence to the model proposed above. Another way to prove that the dissolved oxygen is responsible for the etching process would be the absence of pore formation when using a nonaqueous nonpolar organic electrolyte, which typically does not contain dissolved oxygen. Results from such experiments are presently not available. Furthermore, samples covered with a continuous gold layer with a thickness of approximately 3 nm showed no pore formation even in the presence of dissolved oxygen. The reason for this can be derived from the model presented above. Although the reaction at the cathodic site is still possible the anodic dissolution of silicon is suppressed due to the gold layer which avoids a direct contact between the silicon and the HF solution.

In our proposed etching mechanism expressed in the reactions described in eq 2 the catalytic reaction at the cathodic site is needed for the electron transfer from the gold into the solution which results in an injection of holes into the valence band of silicon. The holes diffuse in silicon to areas which are not covered by the gold film and promote the silicon dissolution at the interface between silicon and HF solution. This explains also why the pore formation at the samples with the discontinuous gold film occurred mostly at the edges of the gold droplets.

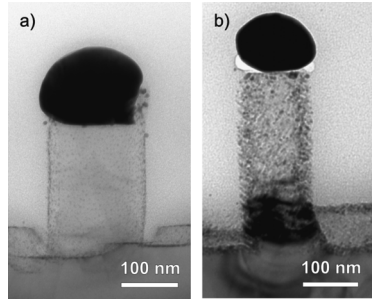

Figure 3. Comparison of (a) a nanowire after HF-treatment with oxygen removal and (b) with oxygen in the HF-solution. Etching in 5 wt % HF for 3 min. The dissolved oxygen in the HF solution is responsible for the corrosion effects.

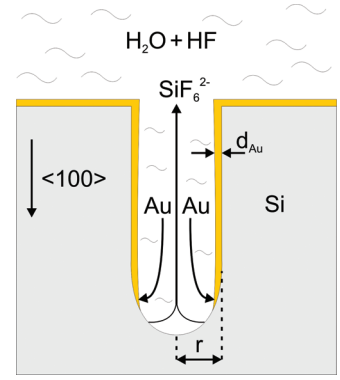

Figure 4. Schematic of the model for explaining the observation of a critical radius for the etched pores. For simplicity here it is assumed that the surface orientation is (100) and that the pore grows perpendicular to the surface.

In comparison to the results reported by Li and Bohn[12] the porosity in our case is significantly lower. Furthermore, our pores are very uniform in diameter. As mentioned above we speculate that the pore walls are covered by a thin layer of gold (in the order of a monolayer). Hence, the silicon is exposed to the electrolyte and dissolved only at the pore tip. Another hint that the pore walls must be passivated comes from the absence of spiking side pores branching off from the main pore which is typical for mesopore growth in silicon.[10]

The proposed pore wall passivation by a gold layer requires transport of the gold in balance with the etching speed of silicon. This implies that the pore size is dependent on the reaction kinetics (HF and oxygen concentration, temperature) and on the mass transport of the chemical reactants. However, more investigations are required to establish a dependency between the experimental parameters and the obtained pore morphology. It is quite remarkable that all the pores have the same diameter. A potential and highly speculative model for this behavior can be developed based on a previous model of the formation of silicon carbide nanotubes, which also showed a remarkably uniform diameter during the deposition of SiC on silicon.[16] As shown in the schematic Figure 4 we assume a simplified model that (i) the surface of the pore with the exception of the tip of the pore is covered by a thin layer of gold or gold-rich silicon, which still has to be proven experimentally as mentioned above. (ii) This surface layer grows with the speed of the pore etching and the gold is supplied continuously from the solution *via* diffusion from the top of the pore. This leads to a growth speed v_{Au} of the deposition of the gold layer assuming a diffusivity D_{Au}, a concentration difference Δc_{Au}, and a length

l of the pore as well as a thickness d_{Au} of the gold layer with a volume density n_{Au} of gold in the coverage:

$$v_{Au} = \frac{D_{Au} r}{2 d_{Au} n_{Au}} \frac{\Delta c_{Au}}{l} \quad (3)$$

where r is the pore radius. Since the assumed gold layer will have a thickness in the monolayer range only (*i.e.*, < 1 nm), in the calculation the radius of the silicon pore (without gold coverage) and that of the open pore in the presence of the gold coverage is approximately taken as equal to simplify the equations.

(iii) The transport of etched away silicon from the bottom of the pore to the top of the pore is accomplished by the slowest process of the possible three processes, diffusion of oxygen to the pore tip, diffusion of HF to the tip, or diffusion of the etching product SiF_6^{2-} from the bottom to the top of the pore. Although presently it is not clear which of these three diffusion processes is rate limiting, the functional form will be the same in all cases. Here we write the resulting etching velocity v_{etch} as a function of the slowest species involved in the etching process with a concentration difference of Δc_{etch} between the bottom and the top of the pore. We assume a diffusion coefficient D_{etch} and get then to

$$v_{etch} = \frac{D_{etch}}{n_{Si}} \frac{\Delta c_{etch}}{l} \quad (4)$$

where n_{Si} is the volume density of silicon atoms in silicon. Here we also have assumed as in the case of the derivation of eq 3 that the radius of the silicon pore (without gold coverage) and that of the open pore in the presence of the gold coverage is approximately taken as equal to simplify the equations.

Since for a steady state etching process the two velocities have to be identical, it is obvious that this can only happen for a critical pore radius r_{crit} given by

$$r_{crit} = \frac{\Delta c_{etch}}{\Delta c_{Au}} \frac{2 d_{Au} n_{Au}}{n_{Si}} \frac{D_{etch}}{D_{Au}} \quad (5)$$

This highly speculative model would explain why all the pores have the same radius. On the basis of eq 5 it can also be expected that this critical radius can be influenced by the oxygen concentration or the HF concentration and the temperature *via* the temperature dependence of the ratio of the involved diffusion coefficients.

We could prove that the well-known mechanism of catalytic etching of silicon by metals[13,14,17] does not apply for our experiments since no gold was found at the pore tips and the diameter of the pores does not correlate with the size of the gold droplets above.

Let us mention for completeness that for experiments where a passivation *via* HF is needed without a pore formation, the gold needs to be removed from the surface. We recognized that the little gold clusters at the surface of the MBE grown nanowires cannot be removed *via* the standard gold etchants like *aqua regia* or $KI + I_2 + H_2O$. Larger gold droplets can be dissolved with those etchants easily. We developed a method to remove the tiny gold clusters. First the big gold droplet on top of the nanowire, which is required for the VLS growth, was removed *via* a $KI + I_2$ solution. This solution consisted of 20 g of KI, 5 g of I_2, and 100 mL of H_2O. The sample was put into the solution for 5 min. Next, the sample was annealed in nitrogen (also argon is possible) at 750 °C for 3 h. This annealing leads to an agglomeration of the gold clusters. Finally the sample was treated again in the $KI + I_2$ solution. Subsequently, the samples were again dipped in HF and also treated with the $KI + I_2$ solution again in order to make sure that all gold is removed. After this treatment the nanowires do not look as corroded as without the treatment. However, a few pores are still visible. The gold is now completely removed from the surface of the nanowires, see Figure 5.

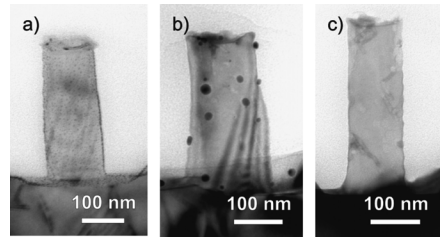

Figure 5. SEM images taken at three different steps during the complete gold removal of MBE-grown silicon nanowires: (a) after removal of the gold droplet on top of the nanowire with $KI + I_2 + H_2O$, (b) after annealing at 750 °C for 3 h, (c) after treatment with $KI + I_2 + H_2O$ and HF dip.

CONCLUSIONS

In our experiments with gold-decorated nanowires we observed a pore formation after treatment in aqueous HF solution. From TEM investigations we noticed a pore formation exclusively in the ⟨100⟩ direction of the silicon nanowires. The same results were found for planar silicon samples covered by a discontinuous thin layer of gold. Because of the directed pore formation in ⟨100⟩ direction which occurs under a certain angle to the ⟨111⟩ oriented surface a divalent dissolution reaction is expected. Furthermore, the dissolved oxygen in the solution was proven to be necessary for the pore formation because of its catalytic reaction at the cathodic site formed by the gold clusters. From these results we proposed a tentative model predicting a constant diameter for all pores and involving a combination of divalent silicon dissolution and metal-assisted charge carrier injection into silicon. The model is highly speculative since it requires the presence of a thin gold layer at the pore walls which cannot yet be shown unambiguously based on TEM investigations. The pore formation procedure reported in this paper could potentially be applicable for the controlled etching of porous structures with uniform pore diameters in the range of only a few nanometers.

EXPERIMENTAL SECTION

Undoped single crystalline ⟨111⟩ silicon nanowires were grown *via* the vapor−liquid−solid (VLS) mechanism in an MBE-chamber at a temperature of 525 °C and a pressure of 10^{-9} mbar.[18] First, the gold is evaporated until the desired thickness of 2 nm onto a ⟨111⟩ oriented substrate. Because of the high temperature, the establishing alloy forms droplets. In the next step silicon is evaporated. The silicon atoms adsorb at the droplet because of its high adsorption coefficient which is close to 1.[19] The atoms saturate the droplet and form a eutectic. At the droplet/silicon interface silicon precipitates and crystallizes in the form of an epitaxial nanowire. MBE-grown silicon nanowires usually have a low aspect ratio with diameters between 100 and 160 nm and lengths between 100 and 500 nm. Gold forms a wetting layer at the surface of silicon at the temperatures used for the growth. During the growth also the cylindrical surfaces of the nanowires are covered by a thin wetting layer of gold. When the silicon wafer is cooled down, the gold layer disintegrates into tiny gold clusters with diameters up to 4 nm.

A typical example of an MBE-grown silicon nanowire can be seen in the cross-sectional transmission electron microscope (TEM) picture in Figure 1a. A ⟨111⟩ silicon wire grew perpendicular to the ⟨111⟩ oriented substrate. At the tip the gold droplet is visible, represented by the dark area in the TEM picture. The gold is required for the VLS growth process. On the cylindrical wall the tiny gold clusters are visible as mentioned above.

In addition to using the just described silicon nanowire samples, gold-assisted etching was also investigated for planar surfaces. (111) Silicon wafers with a thin layer of gold (approximately 3 nm *via* sputter deposition) were heated at 750 °C for 3 h in a nitrogen atmosphere. This annealing leads to gold droplet formation. Subsequently, both the nanowire and the silicon wafer samples were treated with 5 wt % HF for 3 min. After this procedure the samples were investigated by TEM.

Acknowledgment. We thank DFG and the cluster of Excellence of the State of Saxony-Anhalt for financial support.

REFERENCES AND NOTES

1. Yablonovitch, E. Inhibited Spontaneous Emission in Solid-State Physics and Electronics. *Phys. Rev. Lett.* **1987**, *58*, 2059–2062.
2. John, S. Strong Localization of Photons in Certain Disordered Dielectric Superlattices. *Phys. Rev. Lett.* **1987**, *58*, 2486–2489.
3. Birner, A.; Wehrspohn, R. B.; Gösele, U. M.; Busch, K. Silicon-Based Photonic Crystals. *Adv. Mater.* **2001**, *13*, 377–388.
4. Matthias, S.; Müller, F.; Jamois, C.; Wehrspohn, R. B.; Gösele, U. Large-Area Three-Dimensional Structuring by Electrochemical Etching and Lithography. *Adv. Mater.* **2004**, *16*, 2166–2170.
5. Anglin, E. J.; Cheng, L.; Freeman, W. R.; Sailor, M. J. Porous Silicon in Drug Delivery Devices and Materials. *Adv. Drug Delivery Rev.* **2008**, *60*, 1266–1277.
6. Rumpf, K.; Granitzer, P.; Pölt, P.; Reichmann, A.; Krenn, H. Structural and Magnetic Characterization of Ni-filled Porous Silicon. *Thin Solid Films* **2006**, *515*, 716–720.
7. Langner, A.; Knez, M.; Müller, F.; Gösele, U. TiO_2 Microstructures by Inversion of Macroporous Silicon Using Atomic Layer Deposition. *Appl. Phys. A* **2008**, *93*, 399–403.
8. Lehmann, V.; Föll, H. Formation Mechanism and Properties of Electrochemically Etched Trenches in n-Type Silicon. *J. Electrochem. Soc.* **1990**, *137*, 653–659.
9. Lehmann, V. The Physics of Macropore Formation in Low Doped n-Type Silicon. *J. Electrochem. Soc.* **1993**, *140*, 2836–2843.
10. Lehmann, V. *Electrochemistry of Silicon;* Wiley VCH: New York, 2002.
11. Smith, R. L.; Collins, S. D. Porous Silicon Formation Mechanisms. *J. Appl. Phys.* **1992**, *71*, R1–R22.
12. Li, X.; Bohn, P. W. Metal-Assisted Chemical Etching in HF/H_2O_2 Produces Porous Silicon. *Appl. Phys. Lett.* **2000**, *77*, 2572–2574.
13. Huang, Z.; Fang, H.; Zhu, J. Fabrication of Silicon Nanowire Arrays with Controlled Diameter, Length, and Density. *Adv. Mater.* **2007**, *19*, 744–748.
14. Huang, Z.; Zhang, X.; Reiche, M.; Liu, L.; Lee, W.; Shimizu, T.; Senz, S.; Gösele, U. Extended Arrays of Vertically Aligned Sub-10 nm Diameter [100] Si Nanowires by Metal-Assisted Chemical Etching. *Nano Lett.* **2008**, *8*, 3046–3051.
15. Christophersen, M.; Carstensen, J.; Feuerhake, A.; Föll, H. Crystal Orientation and Electrolyte Dependence for Macropore Nucleation and Stable Growth on p-Type Si. *Mater. Sci. Eng., B* **2000**, *69−70*, 194–198.
16. Scholz, R.; Gösele, U.; Niemann, E.; Wischmeyer, F. Micropipes and Voids at β-SiC/Si(100) Interfaces: An Electron Microscopy Study. *Appl. Phys. A* **1997**, *64*, 115–125.
17. Peng, K.; Zhang, M.; Lu, A.; Wong, N.-B.; Zhang, R.; Lee, S.-T. Ordered Silicon Nanowire Arrays *via* Nanosphere Lithography and Metal-Induced Etching. *Appl. Phys. Lett.* **2007**, *90*, 163123.
18. Schubert, L.; Werner, P.; Zakharov, N. D.; Gerth, G.; Kolb, F. M.; Long, L.; Gösele, U.; Tan, T. Y. Silicon Nanowhiskers Grown on ⟨111⟩ Si Substrates by Molecular-Beam Epitaxy. *Appl. Phys. Lett.* **2004**, *84*, 4968–4970.
19. Wagner, R. S.; Ellis, W. C. The Vapor−Liquid−Solid Mechanism of Crystal Growth and Its Application to Silicon. *Trans. Met. Soc. AIME* **1965**, *233*, 1053–1064.